CHAPTER V

PHASE FORMATION, MICROSTRUCTURE AND ELECTRICAL PROPERTIES OF $Ba(Zr_xTi_{1-x})O_3$ CERAMICS SYNTHESIZED THROUGH A NOVEL COMBUSTION TECHNIQUE

Introduction

Barium titanate (BT) ceramics have been used extensively as electroceramics materials due to thier high dielectric constant and low dielectric loss. The phase transformations of BT occur at 120 °C, 0 °C and -90 °C from cubic to tetragonal, tetragonal to orthorhombic and orthorhombic to rhombohedral, respectively [25].The dropping in maximum dielectric constant is accompanied with the phase transformation at lower temperature [8].

$Ba(Zr_xTi_{1-x})O_3$ (BZT) system, one of the first $BaTiO_3$-based solid solution, has been chosen in the fabrications of ceramic capacitors because Zr^{4+} is chemically more stable than Ti^{4+}. Moreover, Zr-substitution at Ti-site has been found to be an effective way to decrease the Curie temperature and exhibits several interesting features in the dielectric behavior and phase formation of $BaTiO_3$ ceramics. The Zr-ion substitution affects an increase of rhombohedral to orthorhombic ($T_{r\text{-}o}$) and orthorhombic to tetragonal ($T_{o\text{-}t}$) phase transition temperature but decreases the tetragonal to cubic (T_c) phase transition temperature. The pinch phase transitions between three phase transitions merge into one peak where $x \leq 0.15$ [10, 30]. Below 15 mol% zirconium, there are several difference reports about the effects of zirconium substituted on phase formation and dielectric properties of BZT. In term of structural phase, some researchers distinguished BZT belonging to tetragonal structure [6, 10, 31] and the tetragonality was decreased by increasing zirconium content [6, 31]. While several literatures reported that the amount of orthorhombic to rhombohedral phase transformation was increased with increasing zirconium [8, 9, 10]. In term of dielectric properties, Huang, et al. [31] explained maximum dielectric constant was enhanced by increasing the amount of zirconium. On the other hand, Chen, et al. [6] reported the maximum dielectric constant was depressed by the amount of zirconium substitution.

Kuang, et al. [8] represented the highest maximum dielectric exhibited in BZT with x = 0.08. For BZT with x less than 0.08, maximum dielectric constant insignificantly relate to the amount zirconium and the maximum dielectric constant tended to increase with increasing zirconium content is observed in BZT with $x \geq 0.8$.

Due to the variation in reports, an accurate investigation of the zirconium content effects on phase formation and dielectric properties in BZT is topical. In addition, our previous work has demonstrated that high quality BZT ceramics can be produced via the combustion technique. Therefore, this study aims to synthesize $Ba(Zr_xTi_{1-x})O_3$ (BZT, $0.025 \leq x \leq 0.150$, step = 0.025) ceramics by the combustion technique. The effect of composition on phase formation, dielectric and ferroelectric properties of BZT was extensively investigated.

Experimental procedure

$Ba(Zr_xTi_{1-x})O_3$ ceramics were prepared via the combustion technique using urea as fuel. The starting materials barium carbonate ($BaCO_3$), zirconium dioxide (ZrO_2) and titanium dioxide (TiO_2) were weighed based on the stoichiometric compositions of $Ba(Zr_xTi_{1-x})O_3$ (BZT100x, $0.025 \leq x \leq 0.150$, step = 0.025). The weighed raw materials were mixed by ball milling with zirconia media in ethanol for 24 h, and then were dried and the powders were ground using an agate mortar and sieved into a fine powder. The mixed powders and urea (CH_4N_2O) were mixed with a ratio of 1:2 in an agate mortar. All compositions were calcined at 1000 °C for 5 h [8]. The calcined ones were again ball-milled in the mixture medium absolute ethanol for 24 h. Disc-shaped specimens with 15 mm in diameter were fabricated using a hydraulic pressing and then the green body were sintered at 1375 °C with soaking time at 2 h [8]. The phase formation behavior and the lattice refinement of all compositions were studied by XRD analytical technique. The SEM and TEM were used to study the microstructure of prepared samples. The bulk densities of the sintered samples were measured by the Archimedes method. The temperature dependence of relative permittivity and dielectric loss of BZT specimens was investigated using LCR meter. The measurement of ferroelectric hysteresis loops was conducted at room temperature by using a ferroelectric tester.

Chemical compositions reaction

$$BaCO_3 + xZrO_2 + (1-x)TiO_2 \rightarrow Ba(Zr_xTi_{1-x})O_3 + CO_2 \qquad \text{[Eq. 25]}$$

Results and discussion

The X-ray diffractograms of $Ba(Zr_xTi_{1-x})O_3$ powders calcined at 1000 °C for 5 h with various x values from 0.025 to 0.150 are shown in Figure 49. All diffraction peaks showed a pure perovskite structure. The calcined temperature of combustion technique was lower than solid state reaction method ~200 °C, indicating the energy released from the combustion reaction of the fuel [6].

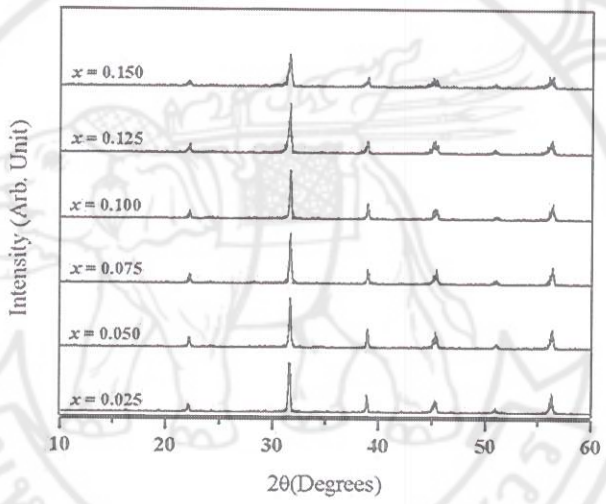

Figure 49 XRD patterns of $Ba(Zr_xTi_{1-x})O_3$ powders with $0.025 \leq x \leq 0.150$

The morphologies of BZT calcined powders were observed by SEM photographs and TEM micrographs which are also shown in Figure 50. The morphologies observed from SEM exhibited spherical shape with agglomerated form although they were shaken by ultrasonic agitation. This phenomenon demonstrated that the combustion technique preparation produced the strong inter-particle forces in calcined powders. This can be explained by the liquid environment, which is occurred during the decomposed processes of urea, assisted the particles to be closely and easier to reacted [47, 48]. The average particle of calcined powders is in the range of 239-471 nm. The TEM observations confirmed the morphology of the prepared powders

showing spherical shape with agglomerated formed (Figure 51). It could be also seen that many fine particles with a nanosize existed.

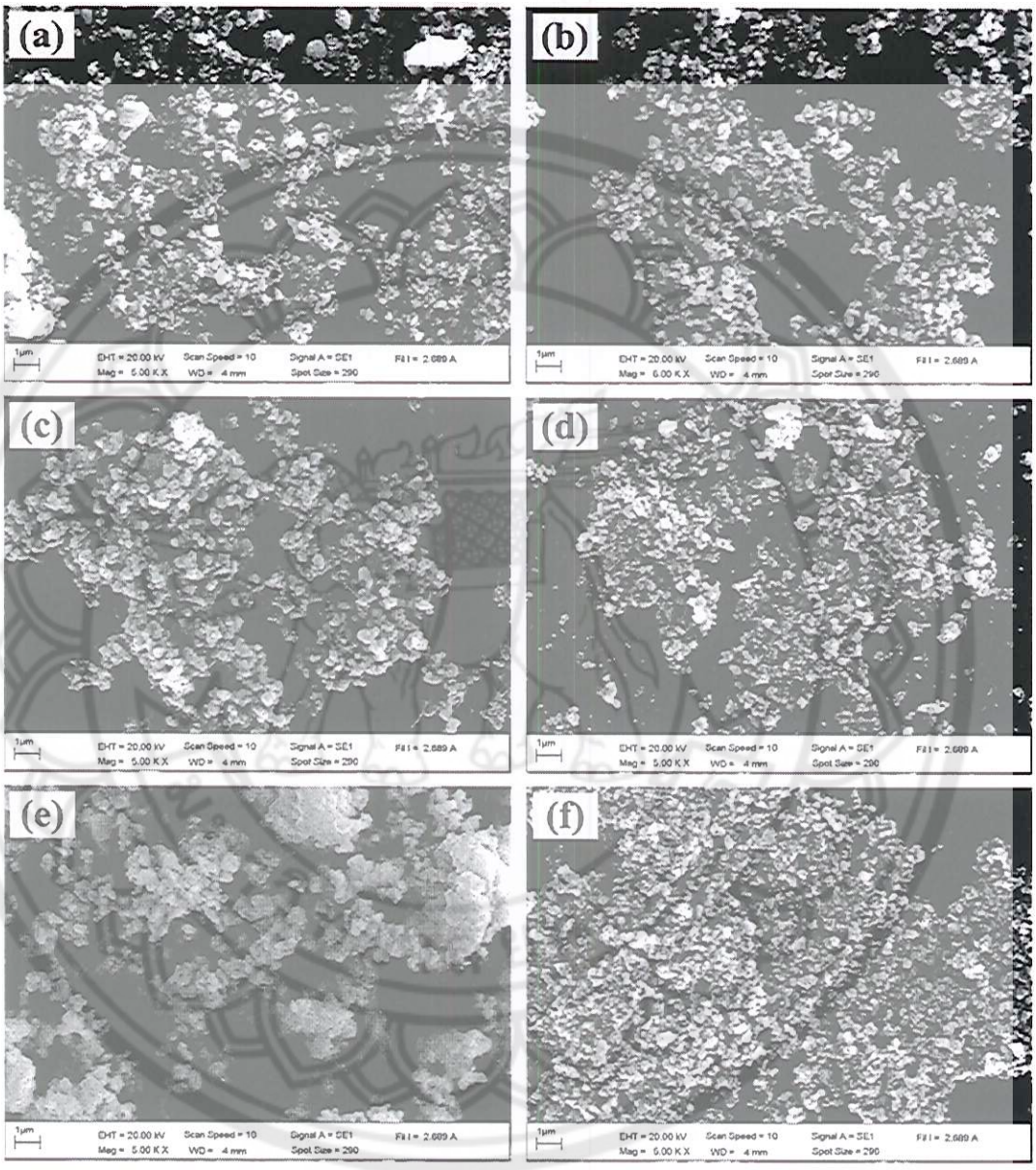

Figure 50 SEM photographs of $Ba(Zr_xTi_{1-x})O_3$ calcined powders; (a) $x = 0.025$, (b) $x = 0.050$, (c) $x = 0.075$, (d) $x = 0.100$, (e) $x = 0.125$ and (f) $x = 0.150$

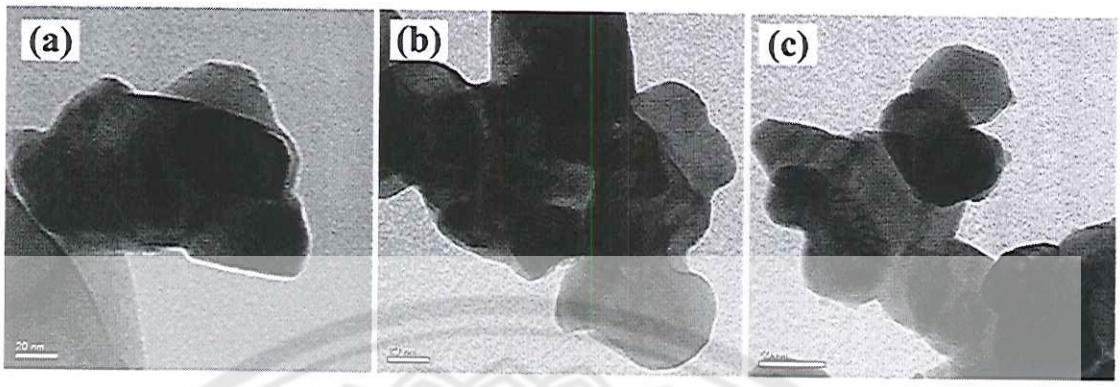

Figure 51 TEM images of $Ba(Zr_xTi_{1-x})O_3$ calcined powders; (a) $x = 0.050$, (b) $x = 0.100$ and (c) $x = 0.150$

The calcined powders were fabricated to be the pellets and sintered at 1375°C for 2 h. The phase formation of BZT ceramics were studied using XRD patterns as shown in Figure 52 and the results showed pure perovskite phase was found in all sintered samples (Figure 52(a)). To determine the phase formation behavior of BZT with increasing the zirconium content, the XRD patterns which measured from 72 to 77° at a very low scanning rate (step size 0.00116 °, time/θ 7.42 s, scan speed 0.05152° /s) were investigated (Figure 52(b)). It can be seen that the diffraction angle also decreases as the zirconium content is raised. This can be explained by the ionic radius of Zr^{4+} (0.072 nm) being larger than Ti^{4+} (0.061 nm), so more substitution of Zr^{4+} will increase the *d* spacing of BZT and cause the diffraction peaks to shift toward a lower angle [4]. At room temperature, the splitting of (133) and (311) diffraction peaks of BZT2.5 ceramics confirms the orthorhombic phase (Refer to ICDD No.01-0812196). When zirconium content was increased to 5 mol%, the two diffraction peaks gradually merged into one peak which was indicated by the rhombohedral phase which was initially diffuse and influenced the phase system (Refer to ICCD No. 01-0850368). The diffraction peak exhibited a sharper curve and a nearly symmetric shape, lightly skewed to the right side in BZT7.5. This implies that the tetragonal phase was occurred and slightly diffused in rhombohedral phase of BZT system (Refer to ICCD No. 00-0030725). When zirconium content was increased to 10 mol%, the distinct non-symmetry (skewed to the right side) of the diffraction peak can be explained by the BZT showing a tetragonal phase. Moreover, when zirconium content was higher

than 10 mol%, the diffraction peak changed from non-symmetry to near symmetry illustrated the cubic phase influence on BZT system (Refer to ICCD No. 01-0741961). The accurate interpretation is derived from high quality samples which were produced via the combustion technique.

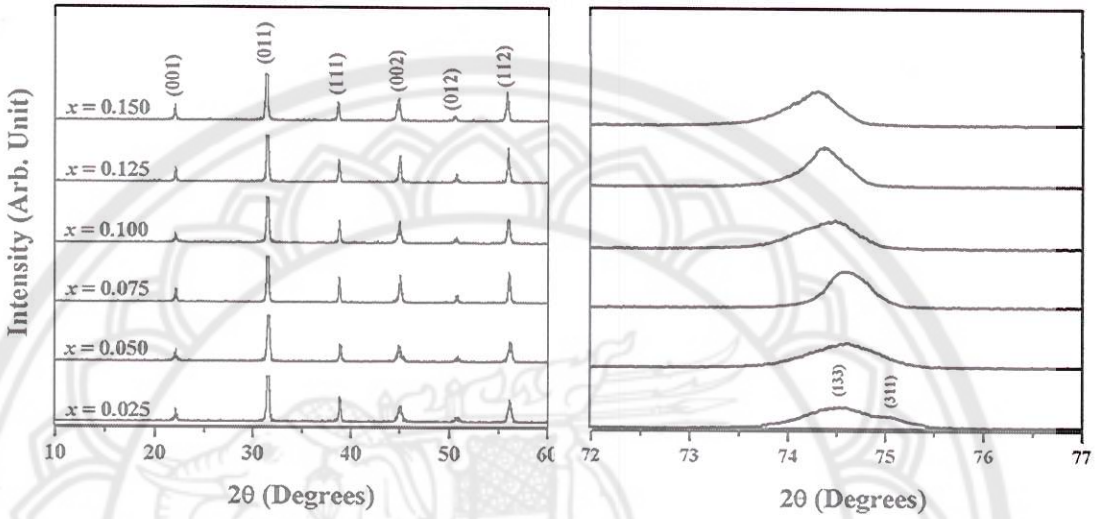

Figure 52 XRD patterns of $Ba(Zr_xTi_{1-x})O_3$ ceramics with $0.025 \leq x \leq 0.150$; (a) at 2θ of 10-60° and (b) slow scanning rate at 2θ of 72-77°

The effect of zirconium content on the grain size of BZT ceramics is shown in Figure 53. By increasing the zirconium content, there was a noticeable an accretion of the grain size and reduction in the grain size distribution. The grain size tended to increase from 1.54 - 4.70 μm when zirconium content is raised (Table 12). Dixit, et al. [30] revealed that the morphology feature of BZT appears to be quite sensitive to the zirconium content. They proposed that beyond 20 mol% zirconium content, the grain size increased with more uniform in grain size distribution due to cubic phase content increased.

The measured density with a variation in zirconium content of BZT is listed in Table 12. The density of the ceramics was in the range of 5.61–5.86 g/cm^3 and the densities insignificantly changed with zirconium content modification. The highest density exhibited in BZT12.5 was 97% of the theoretical density and was higher than the samples which were prepared via the solid-state reaction method [10] and the wet chemical reaction method [9].

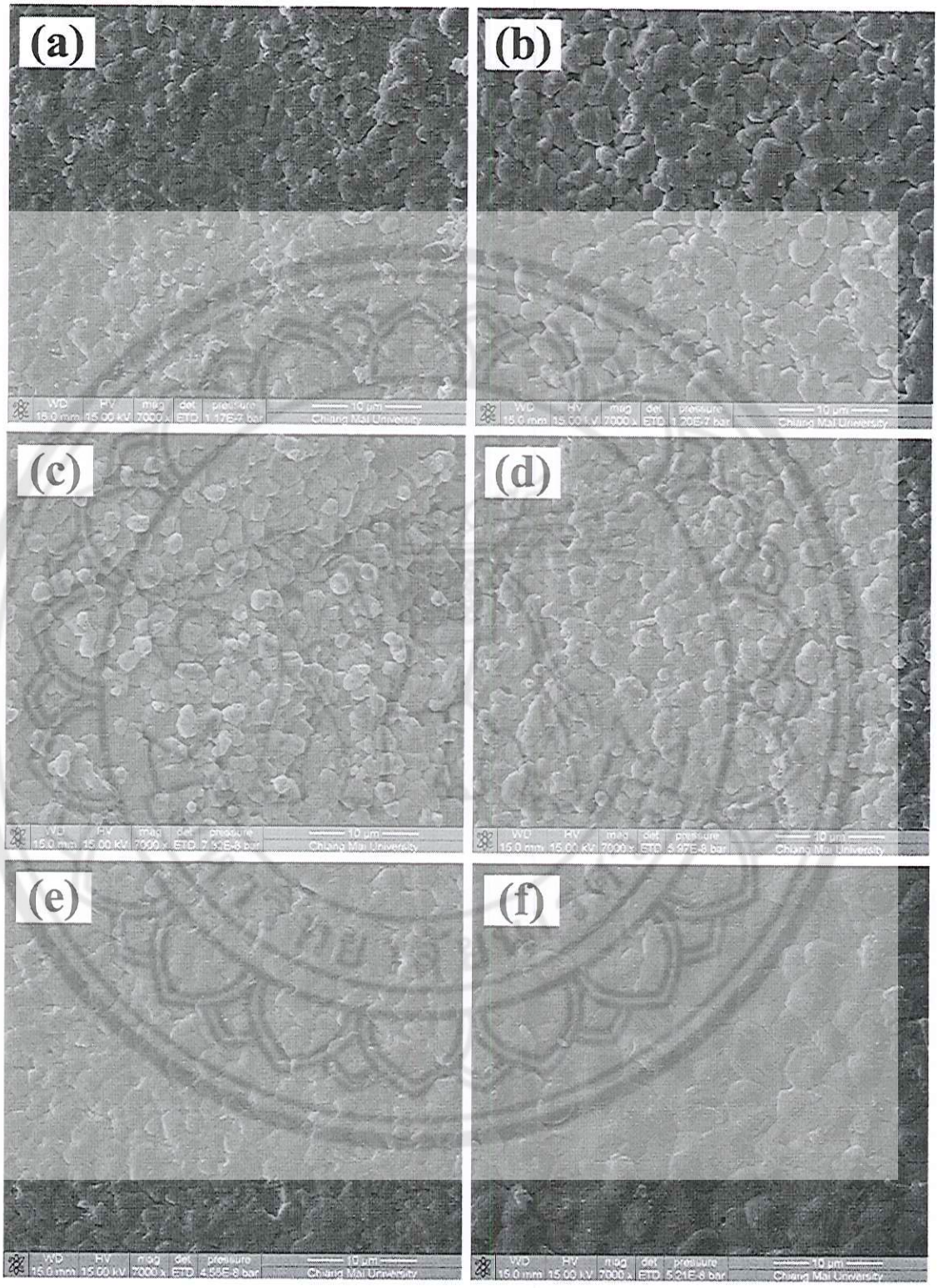

Figure 53 The SEM micrographs of $Ba(Zr_xTi_{1-x})O_3$ sintered ceramics; (a) $x = 0.025$, (b) $x = 0.050$, (c) $x = 0.075$, (d) $x = 0.100$, (e) $x = 0.125$ and (f) $x = 0.150$

Table 12 Average grain size and density of $Ba(Zr_xTi_{1-x})O_3$ sintered ceramics

Composition of x	Average grain size (μm)	Density (g/cm^3)
$x = 0.025$	1.54	5.69
$x = 0.050$	1.66	5.64
$x = 0.075$	2.62	5.61
$x = 0.100$	2.59	5.78
$x = 0.125$	3.04	5.86
$x = 0.150$	4.70	5.75

The temperature dependence of the dielectric constant of BZT ceramics with various stoichiometric percentage of zirconium is shown in Figure 54. It was found that as zirconium increased from 2.5 to 5.0 mol%, maximum dielectric constant tended to increase. The reduction of maximum dielectric constant appeared in BZT with 7.5 mol% zirconium. Thereafter, more zirconium doping induced the increasing of maximum dielectric constant again. The increasing of maximum dielectric constant reached maximum value in BZT12.5 thereafter, it decreased in BZT15. The maximum dielectric constant and the loss tangent at Curie point were listed in Table 13. The value of density and maximum dielectric constant of BZT in all compositions in this study were higher when compared to previous works [6, 9, 10, 33] which indicated that high quality BZT ceramics could be prepared via the combustion technique.

The transition temperature from orthorhombic to tetragonal structure (T_{o-t}) is obviously observed in BZT2.5, BZT5.0 and BZT7.5 ceramics. The dielectric peak at T_{o-t} appeared broader with increasing zirconium content. From literature surveyed, by increasing x, T_{r-o} (transition temperature from rhombohedral to orthorhombic structure) and T_{o-t} peaks were shifted to higher temperatures. However, the shifted rate of T_{r-o} peak is higher than that of T_{o-t} peak and two peaks were nearly merged at around x of 0.08 [10]. Therefore, the broadening of dielectric curve at T_{o-t} is caused from higher diffusive T_{r-o} peak by increased amount of zirconium.

The phase transition temperature $T_{o\text{-}t}$ (exhibited at lower temperature) and the Curie temperature (T_c) (exhibited at higher temperature) were observed from dielectric loss peak (Figure 55) and are listed in Table 13.

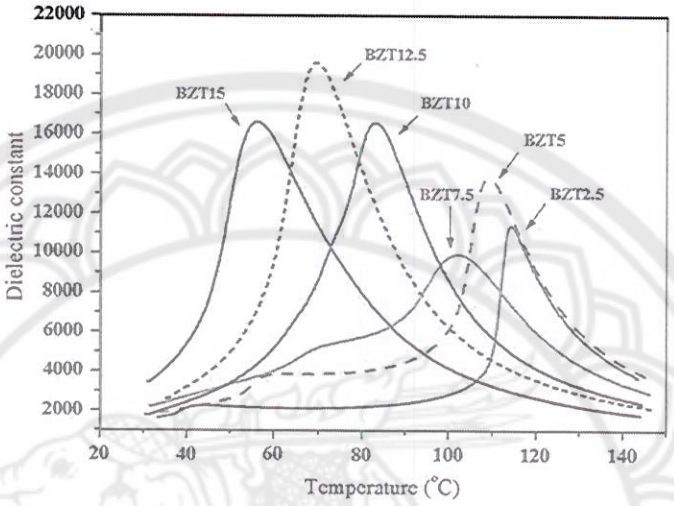

Figure 54 Temperature dependences of dielectric constant of BZT100x ceramics where $0.025 \leq x \leq 0.150$

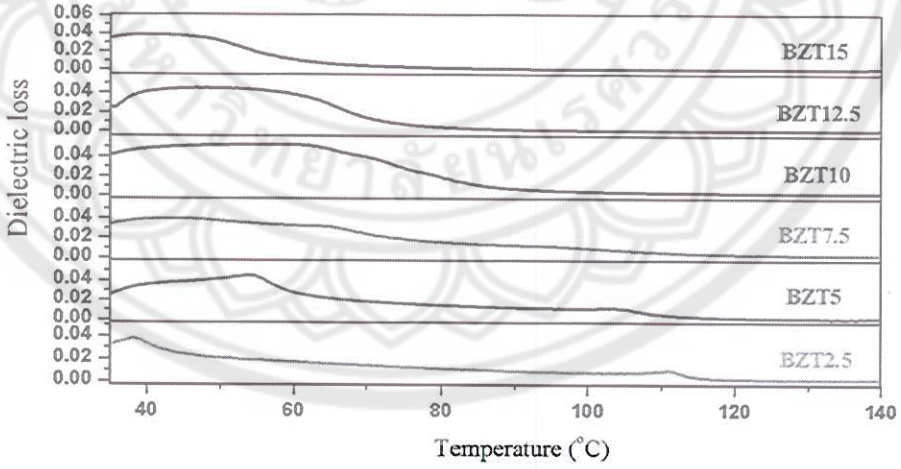

Figure 55 Dielectric loss curve of the BZT100x ceramics where $0.025 \leq x \leq 0.150$

To investigate the pinch phase transition characteristic, the phase transition temperature $T_{o\text{-}t}$ and T_c as function of zirconium doping content were plotted (Figure 56). It is found that the increase of $T_{o\text{-}t}$ and decrease of T_c showed nonlinear function with increasing zirconium content. The intersection of $T_{o\text{-}t}$ and T_c phase transitions temperature was observed at around 9.4 mol% of zirconium which displays the two phase transition is pinched into one dielectric peak due to the increased Zr content. Moreover, the function plotted revealed that the interval between $T_{o\text{-}t}$ and T_c tended to decrease by increasing zirconium content.

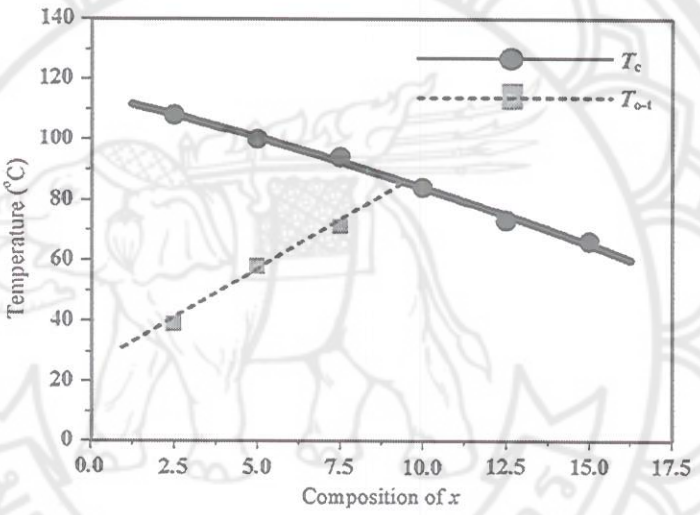

Figure 56 Phase transition temperature $T_{o\text{-}t}$ and T_c as function of zirconium content x for $Ba(Zr_xTi_{1-x})O_3$ ceramics

The study of phase transition characteristic exposed the increase and decrease of maximum dielectric constant and broadening of dielectric curve in dielectric result. In this study, BZT with zirconium $0.025 \leq x \leq 0.075$ showed lower maximum dielectric constant compared with BZT with zirconium $0.100 \leq x \leq 0.150$. This can be related to the orthorhombic phase influences on dielectric constant. In case of BZT with 7.5 mol% zirconium, the lowest of maximum dielectric constant with broadest dielectric curve was exhibited. This may be attributed to the rhombohedral phase being the highest diffused as exhibited in the XRD result. Maximum dielectric constant was enhanced immediately again in the BZT sample with zirconium content

10 mol% and reached the highest in BZT with 12.5 mol% zirconium. This demonstrated that tetragonal phase induces increasing dielectric constant. The reduction of BZT with 15 mol% zirconium could be speculated by the cubic phase affected.

A diffuse phase transition is generally characterized by the diffuseness of phase transition (γ) which was calculated from a modified Curie–Weiss law [66] as shown in the Figure 57. The γ values of the BZT prepared via the combustion technique are in the range of 1.32 to 1.95 upon zirconium content as listed in Table 13. The diffuseness was increased when zirconium content increased and reached its highest diffuseness of 1.95 on BZT7.5. This result was supported by two reasons. The first one is the diffusion between $T_{r\text{-}o}$ and $T_{o\text{-}t}$ arouse dielectric curve to broader. Another one reason is the reducing of the interval between $T_{o\text{-}t}$ and T_c which indicated the phase transition at $T_{o\text{-}t}$ and T_c more easily diffused. After reaching the highest value, the diffuseness decreased in BZT10 and increased again in BZT12.5 and BZT15. The increment of the γ with increasing zirconium content can be explained by the diffusive phase transition between ferroelectric to paraelectric phase. This result is consistent with the XRD result and the report in literature [35, 65, 67].

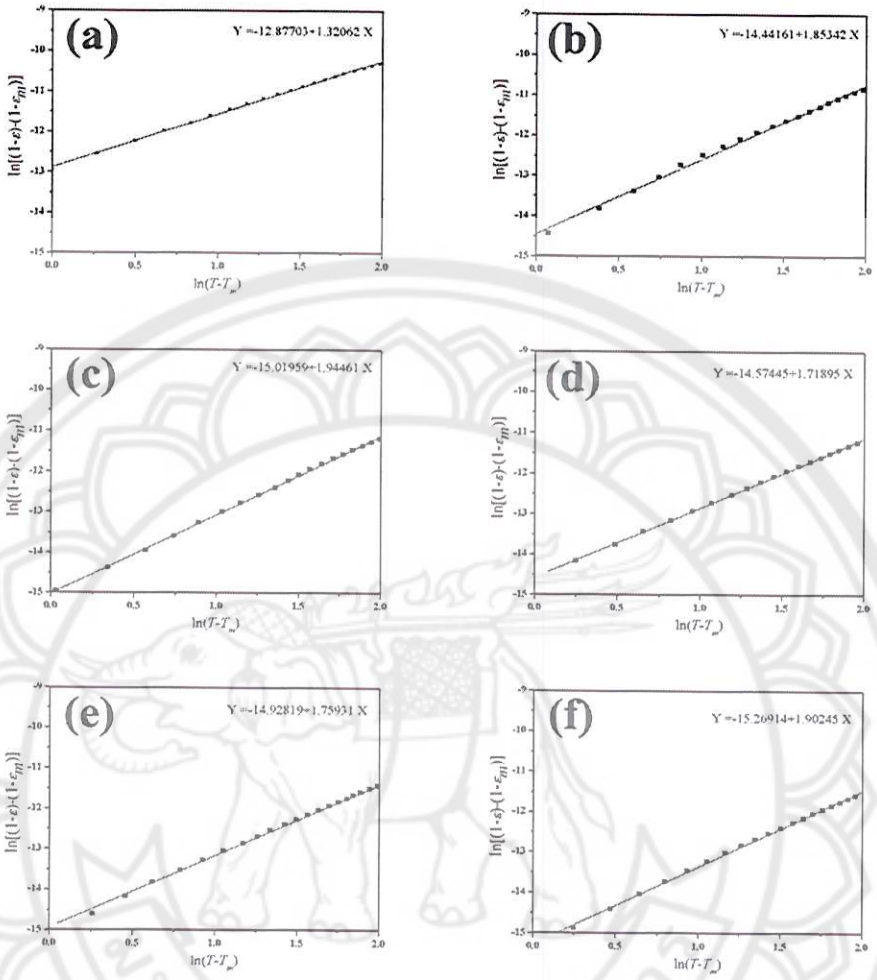

Figure 57 The dependence of $\ln\left(\frac{1}{\varepsilon}-\frac{1}{\varepsilon_m}\right)$ versus $\ln(T-T_m)$ of BZT100x ceramics; (a) $x = 0.025$, (b) $x = 0.050$, (c) $x = 0.075$, (d) $x = 0.100$, (e) $x = 0.125$ and (f) $x = 0.150$

Table 13 The T_{o-t}, T_c, maximum dielectric constant (ε_r) and dielectric loss (tanδ) at T_c, and diffuseness (γ) of $Ba(Zr_xTi_{1-x})O_3$ ceramics

Composition of x	T_{o-t} (°C)	T_c (°C)	Maximum dielectric constant	Dielectric loss at T_c	Diffuseness (γ)
$x = 0.025$	39	108	11,380	0.004	1.32
$x = 0.050$	50	100	13,770	0.006	1.85
$x = 0.075$	71	94	9,930	0.009	1.95
$x = 0.100$	-	84	16,540	0.013	1.72
$x = 0.125$	-	73	19,600	0.015	1.76
$x = 0.150$	-	66	16,600	0.017	1.90

Figure 58 shows the polarization-electric field characteristics of BZT ceramics at room temperature. It is found that well- behaved hysteresis loops can be observed in all compositions of BZT. The hysteresis loop increasingly swelled with increasing amount of zirconium from BZT2.5 to BZT5. In BZT7.5, the altitude of *P–E* loop was decreased and appears slimmer as shown in Figure 58 (a). The loop altitude was raised again in BZT10, and there after the altitude and the slope was decreased with increasing zirconium content (Figure 58 (b)). The remanant polarization (P_r) and the coercive field (E_c) of BZT for all compositions were listed in Table 14. The value of P_r tended to increase as the amount of zirconium then depreciated for BZT7.5. The remanant polarization was raised again in BZT10 thereafter the P_r was found to decrease with increasing zirconium content. The reduction of P_r in BZT7.5 may be due to the diminution of domain wall mobility caused from the mixing phase of rhombohedral and orthorhombic phases. In the case of BZT5, although the diffusion of rhombedral phase did not cause P_r to reduce, it affected the value of E_c which showed the highest. For BZT with $x \geq 10$, remanent polarization tended to decrease with increasing zirconium content. This can be explained by the difference of the radius of

Zr^{4+} and Ti^{4+} [6]. Moreover, the procrastination of Curie temperature approaching to room temperature may cause the decrease of the ferroelectric characteristic [10].

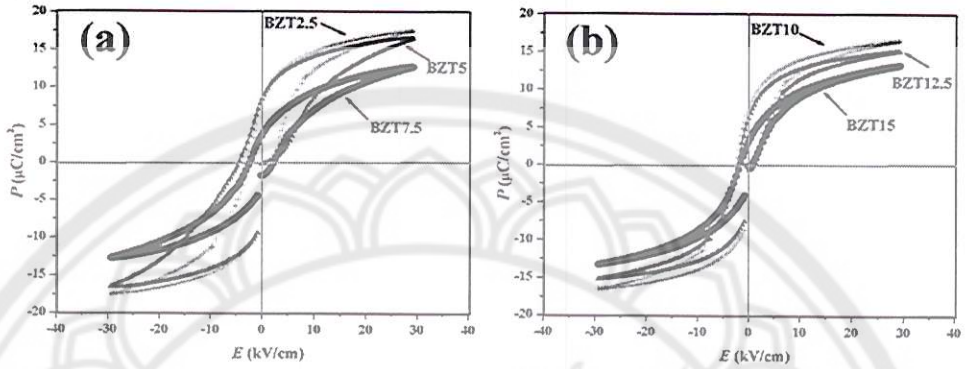

Figure 58 *P–E* hysteresis loop of BZT100x ceramics (a) $0.025 \leq x \leq 0.075$ and (b) $0.100 \leq x \leq 0.150$

Table 14 The P_r and E_c of $Ba(Zr_xTi_{1-x})O_3$ ceramics

Composition of x	P_r ($\mu C/cm^2$)	E_c (kV/cm)
$x = 0.025$	8.31	2.42
$x = 0.050$	8.36	4.51
$x = 0.075$	3.61	2.17
$x = 0.100$	7.27	2.34
$x = 0.125$	6.33	2.11
$x = 0.150$	3.12	1.79

Conclusions

The phase formation, dielectric behavior and ferroelectric properties of $Ba(Zr_xTi_{1-x})O_3$ ceramics with $0.025 \leq x \leq 0.150$ prepared via the combustion technique were investigated. The X-ray diffraction patterns clearly indicated that the transformation from orthorhombic to rhombohedral, tetragonal or cubic phase is dependent on zirconium content. The dielectric measurement indicated that, by increasing the amount of zirconium substituted, $T_{r\text{-}o}$, $T_{o\text{-}t}$ and T_c phase transition peaks were shifted and the pinched phase transition occurred in BZT with zirconium content ~9.4 mol%. The lowest and the highest maximum dielectric constant were 9930 and 19,600 which were exhibited in BZT with x = 0.075 and 0.125, respectively. The diffusion of rhombohedral and tetragonal phase influenced on the decrease and increase of maximum dielectric constant, respectively. In addition, the diffusion of $T_{r\text{-}o}$ to $T_{o\text{-}t}$ dielectric peak and $T_{o\text{-}t}$ to T_c dielectric peak also caused the reduction in maximum dielectric constant of BZT7.5. Ferroelectric properties were decreased by the diffusion of rhombohedral into orthorhombic phase. The result from XRD investigation, the dielectric behavior analysis and the ferroelectric results were consistent with each other, and hence this work demonstrates the potential for the combustion technique in preparing BZT ceramics.